INTERNATIONAL JOURNAL OF SATELLITE COMMUNICATIONS AND NETWORKING
Int. J. Satell. Commun. Network. 2012; **30**:64–75
Published online in Wiley Online Library (wileyonlinelibrary.com). DOI: 10.1002/sat.1006

Improving the spectral efficiency of FDM-CPM systems through packing and multiuser processing[‡]

Amina Piemontese[*,†], Nicolò Mazzali and Giulio Colavolpe

Università di Parma, Dipartimento di Ingegneria dell'Informazione, Viale G. P. Usberti, 181A, I-43124 Parma, Italy

SUMMARY

In frequency division multiplexed (FDM) systems, spectral efficiency (SE) can be increased by reducing the spacing between two adjacent channels, thus increasing the relevant interference and possibly accounting for it at the receiver. In this paper, we consider a FDM system where each user employs a continuous phase modulation, serially concatenated with an outer code through an interleaver, and iterative detection/decoding. We show that, by taking into account the increased interference using properly designed multiuser detection and synchronization schemes, it is possible to implement transmission schemes with unprecedented SE at a price of a limited complexity increase with respect to a classical single-user receiver which neglects the interference. Copyright © 2012 John Wiley & Sons, Ltd.

Received 10 January 2012; Accepted 19 January 2012

KEY WORDS: continuous phase modulations, phase and frequency synchronization, phase noise, adjacent channel interference, iterative detection/decoding

1. INTRODUCTION

Spectral efficiency (SE) of frequency division multiplexed (FDM) systems can be increased by reducing the spacing between two adjacent channels, thus allowing overlap in frequency and hence admitting a certain amount of interference [1,2]. This aspect has been investigated from an information-theoretic point of view for linear [3] as well as continuous phase modulations (CPMs) [4], showing that a significant improvement can be obtained through packing even when at the receiver side a single-user detector is employed. When a multiuser receiver is adopted, the benefits in terms of SE can be even larger and the signals can be packed denser and denser [1–5].

Since, as known, the complexity of the optimal multiuser detector increases exponentially with the number of channels, suboptimal detection schemes are required. In the case of a satellite FDM system using linear modulations, the adoption of reduced-complexity multiuser detection (MUD) algorithms borrowed from the literature on code division multiple access (CDMA) is investigated in [1–3] showing that these techniques work well also in this scenario. Although this is, in principle, possible for CPM systems as well, a new reduced-complexity MUD algorithm for an additive white Gaussian noise (AWGN) channel is derived in [6] based on factor graphs (FGs) and the sum-product algorithm (SPA) [7]. This latter framework, often used in the past to reinterpret known algorithms, is very useful for deriving new detection schemes with an unprecedented complexity/performance trade-off [8–12] or for applications where traditional probabilistic methods fail [13]. In this case, the new algorithm designed in [6] by using this framework outperforms all other suboptimal MUD algorithms both from performance and complexity points of view.

*Correspondence to: Amina Piemontese, Università di Parma, Dipartimento di Ingegneria dell'Informazione, Viale G. P. Usberti, 181A, I-43124 Parma, Italy.
†E-mail: piemontese@tlc.unipr.it
‡The paper was presented in part at the 5th Advanced Satellite Mobile Systems Conference and 11th International Workshop on Signal Processing for Space Communications (ASMS&SPSC 2010), Cagliari, Italy, September 2010. This work is funded by Newtec Cy, Sint-Niklaas, Belgium.

But a denser packing has an impact not only on the detection algorithm. In fact, once satisfactorily suboptimal MUD algorithms are available, other subsystems become critical. In particular, carrier synchronization schemes able to cope with the increased interference must be adopted.

In this paper, we will focus on CPMs, since they are often employed in satellite communications and they have been recently included in the 2nd-generation Digital Video Broadcasting - Return Channel Satellite (DVB-RCS2) standard [14]. CPM signals are appealing for satellite systems for their robustness to non-linearities, stemming from the constant envelope, their claimed power and spectral efficiency, and their recursive nature which allows to employ them in serially concatenated schemes [15,16]. In particular, we will consider CPMs serially concatenated with an outer code through an interleaver, and iterative detection/decoding. After the system model description of Section 2, an information theoretic analysis aimed at finding the optimal spacing between two adjacent channels is described in Section 3. Multiuser processing issues are discussed in Section 4, where we propose reduced-complexity schemes for multiuser detection in the presence of time-varying phase noise (PN), and multiuser data-aided (DA) phase and frequency synchronization schemes. Simulation results are reported in Section 5 and, finally, some conclusions are drawn in Section 6.

2. SYSTEM MODEL

We assume that the channel is shared by U independent users. Without loss of generality, we consider synchronous users, all employing the same modulation format and transmitting at the same power, and a return link satellite channel. The extension to the case of asynchronous users, possibly with different power and modulation formats can be pursued as described in [6]. The adoption of CPMs allows to use cheaper nonlinear amplifiers at the transmitters, which can be driven in saturation and whose effect can be neglected in our analysis. On the other hand, we assume that the on-board satellite amplifier works far from the saturation to avoid distortions on the composite signal—this is a common operating choice for this kind of systems. We assume that each user transmits N symbols and we denote by $\alpha_n^{(u)}$ the symbol transmitted by user u at discrete-time n, which takes on values in the M-ary alphabet $\{\pm 1, \pm 3 \cdots \pm (M-1)\}$. Moreover, $\boldsymbol{\alpha}^{(u)} = \left(\alpha_0^{(u)}, \ldots, \alpha_{N-1}^{(u)}\right)^T$ is the vector of the N symbols transmitted by user u and we also denote $\boldsymbol{\alpha}_n = \left(\alpha_n^{(1)}, \ldots, \alpha_n^{(U)}\right)^T$ and $\boldsymbol{\alpha} = \left(\boldsymbol{\alpha}_0^T, \ldots, \boldsymbol{\alpha}_{N-1}^T\right)^T$.[§] The complex envelope of the received signal can be written as

$$r(t) = \sum_{u=1}^{U} s^{(u)}\left(t, \boldsymbol{\alpha}^{(u)}\right) e^{\jmath\theta^{(u)}(t)} + w(t) \tag{1}$$

where $w(t)$ is a zero-mean circularly symmetric white Gaussian noise process with power spectral density (PSD) $2N_0$ (N_0 assumed perfectly known at the receiver), $\theta^{(u)}(t)$ is the PN affecting user u ($\theta^{(u)}(t)$ and $\theta^{(v)}(t)$ are assumed independent for $u \neq v$), and $s^{(u)}(t, \boldsymbol{\alpha}^{(u)})$ is the CPM information-bearing signal of user u which reads

$$s^{(u)}\left(t, \boldsymbol{\alpha}^{(u)}\right) = \sqrt{\frac{2E_S}{T}} \exp\left\{\jmath 2\pi \left[f^{(u)} t + h \sum_{n=0}^{N-1} \alpha_n^{(u)} q(t - nT)\right]\right\}. \tag{2}$$

In (2), E_S is the energy per information symbol, T the symbol interval, $f^{(u)}$ the difference between the carrier frequency of user u and the frequency assumed as reference for the computation of the complex envelope, $q(t)$ the *phase-smoothing response*, and $h = r/p$ the modulation index (r and p are relatively prime integers). The derivative of the function $q(t)$ is the so-called *frequency pulse* of length L symbol intervals. In the generic time interval $[nT, nT+T)$, the CPM signal of user u is completely defined by symbol $\alpha_n^{(u)}$ and state $\sigma_n^{(u)} = \left(\omega_n^{(u)}, \phi_n^{(u)}\right)$ [17], where

$$\omega_n^{(u)} = \left(\alpha_{n-1}^{(u)}, \alpha_{n-2}^{(u)}, \ldots, \alpha_{n-L+1}^{(u)}\right) \tag{3}$$

[§]In the following, $(\cdot)^T$ denotes transpose and $(\cdot)^H$ transpose conjugate.

DOI: 10.1002/sat

is the correlative state and $\phi_n^{(u)}$, which takes on p values, is the phase state. It can be recursively defined as

$$\phi_n^{(u)} = \left[\phi_{n-1}^{(u)} + \pi h \alpha_{n-L}^{(u)}\right]_{2\pi} \tag{4}$$

being $[\cdot]_{2\pi}$ the "modulo 2π" operator. In the following, we define $\boldsymbol{\sigma}_n = \left(\sigma_n^{(1)}, \ldots, \sigma_n^{(U)}\right)^T$ and $\boldsymbol{\sigma} = \left(\boldsymbol{\sigma}_0^T, \ldots, \boldsymbol{\sigma}_N^T\right)^T$.

An approximated set of sufficient statistics can be obtained by extracting η samples per symbol interval from the received signal prefiltered by means of an analog low-pass filter which leaves unmodified the useful signal and has a vestigial symmetry around $\eta/2T$. The condition on the vestigial symmetry of the analog prefilter ensures that the noise samples are independent and identically distributed (i.i.d.) complex Gaussian random variables with independent components, each with mean zero and variance $\Xi^2 = N_0\eta/T$ [6]. We will denote by $r_{n,m}$ the $m-$ th received sample ($m = 0, 1, \ldots, \eta - 1$) of the n-th symbol interval. Assuming $\theta^{(u)}(t)$ constant over an interval of length T, this sample can be expressed as

$$r_{n,m} = \sum_{u=1}^{U} s_{n,m}^{(u)}\left(\alpha_n^{(u)}, \sigma_n^{(u)}\right) e^{j\theta_n^{(u)}} + w_{n,m} \tag{5}$$

where $\theta_n^{(u)} = \theta^{(u)}(nT)$ and, as mentioned, $\{w_{n,m}\}$ are i.i.d. complex Gaussian noise samples and $s_{n,m}^{(u)}\left(\alpha^{(u)}, \sigma^{(u)}\right)$ (whose dependence on $\alpha^{(u)}$ and $\sigma^{(u)}$ will be omitted in the following when unnecessary) is the contribution of user u to the useful signal component. The random process $\left\{\theta_n^{(u)}\right\}$ is modeled according to a discrete-time Wiener process, whose incremental standard deviation over a symbol interval σ_Δ is known at the receiver [12]. In the following, we will define $\mathbf{r}_n = (r_{n,0}, r_{n,1}, \ldots, r_{n,\eta-1})^T$, $\mathbf{r} = \left(\mathbf{r}_0^T, \mathbf{r}_1^T, \ldots, \mathbf{r}_{N-1}^T\right)^T$ and $\mathbf{s}_n^{(u)} = \left(s_{n,0}^{(u)}, s_{n,1}^{(u)}, \ldots, s_{n,\eta-1}^{(u)}\right)^T$.

3. INFORMATION-THEORETIC ANALYSIS

The ultimate performance limits of FDM-CPM systems and the optimal spacing between adjacent channels can be evaluated through the analysis described in [4] and extended to multiuser detection in [5]. This analysis is based on the computation of information rate (IR) and SE. For this analysis only, we will neglect the presence of PN.

As mentioned, all users are assumed to transmit at the same power, to employ the same modulation format, and to be equally spaced in frequency. Under these conditions, the frequency spacing is a measure of the signal bandwidth and the SE can thus be computed. In order to avoid boundary effects, it is assumed $U \to \infty$. However, for complexity reasons a multiuser detector that assumes the presence of only U' users and treats the other remaining users as additional noise is adopted. In other words, the channel model assumed by the receiver is

$$r(t) = \sum_{u=1}^{U'} s^{(u)}\left(t, \boldsymbol{\alpha}^{(u)}\right) + n(t) \tag{6}$$

where $n(t)$ is a zero-mean circularly-symmetric white Gaussian process with PSD $2(N_0 + N_I)$, N_I being a design parameter optimized through computer simulations [4,5] and whose optimal value is practically independent of the signal-to-noise ratio.

We first evaluate the IR $I(\boldsymbol{\alpha}^{(u)}; \mathbf{r})$ achievable by a receiver designed for the auxiliary channel (6) when the actual channel is that in (1) with $U \to \infty$ [4,5]. The problem is an instance of mismatched decoding [18] and can be solved by means of the simulation-based method described in [19], which only requires the existence of an algorithm for exact maximum a posteriori (MAP) symbol detection over the auxiliary channel (the optimal multiuser MAP symbol detector for U' users over AWGN [6]). Assuming a system with an infinite number of users, the IR $I(\boldsymbol{\alpha}^{(u)}; \mathbf{r})$ does not depend on u and we can focus on a generic user. Moreover, we can define the system bandwidth as the separation between two adjacent channels $F = |f^{(u)} - f^{(u-1)}|$ and use it in the definition of the achievable SE [4,5]

DOI: 10.1002/sat

$$\mathrm{SE} = \frac{1}{FT} I\left(\boldsymbol{\alpha}^{(u)}; \mathbf{r}\right) \quad \left[\frac{\mathrm{b}}{\mathrm{s{\cdot}Hz}}\right]. \tag{7}$$

We remark that the use of the optimal multiuser detector for U' users is necessary to obtain achievable lower bounds on IR and SE. On the other hand, since this optimal multiuser receiver is not interesting for a complexity point of view, in the following we will consider suboptimal reduced-complexity algorithms but still starting from the information-theoretic results on the most efficient modulation formats and the relevant spacings. In addition, we will consider practical coding schemes based on serial concatenation and iterative detection/decoding, and also schemes with $U = U'$ and a limited number of users (at most 5)—spacings, modulation formats, and values of SEs obtained from the information-theoretic analysis still represent a very good guideline for the design of practical systems, as shown in the numerical results. Obviously, some (limited) degradation must be expected.

4. CARRIER SYNCHRONIZATION ALGORITHMS

4.1. Multiuser joint detection and phase synchronization

In the presence of PN, phase synchronization must be performed jointly with detection [8,12]. We describe the extension of the reduced-complexity MUD scheme in [6] to the case of channels affected by PN. This algorithm is obtained by means of some graphical manipulations on the FG representing the joint distribution of the transmitted symbols and the channel phase. We follow the Bayesian approach employed in [12] to design single-user detectors for the PN channel.

We can rewrite the signal of user u highlighting the component that depends on the CPM phase state:

$$s_{n,m}^{(u)}\left(\alpha_n^{(u)}, \sigma_n^{(u)}\right) = \bar{s}_{n,m}^{(u)}\left(\alpha_n^{(u)}, \omega_n^{(u)}\right) e^{\jmath\phi_n^{(u)}}.$$

Defining $\psi_n^{(u)} = \left[\phi_n^{(u)} + \theta_n^{(u)}\right]_{2\pi}$, the received signal (5) can be expressed as

$$r_{n,m} = \sum_{u=1}^{U} \bar{s}_{n,m}^{(u)}\left(\alpha_n^{(u)}, \omega_n^{(u)}\right) e^{\jmath\psi_n^{(u)}} + w_{n,m}. \tag{8}$$

Let us now define $\boldsymbol{\omega}_n = \left(\omega_n^{(1)}, \ldots, \omega_n^{(U)}\right)^T$, $\boldsymbol{\omega} = \left(\boldsymbol{\omega}_0^T, \ldots, \boldsymbol{\omega}_N^T\right)^T$, $\boldsymbol{\psi}_n = \left(\psi_n^{(1)}, \ldots, \psi_n^{(U)}\right)^T$, $\boldsymbol{\psi} = \left(\boldsymbol{\psi}_0^T, \ldots, \boldsymbol{\psi}_N^T\right)^T$, and $\bar{\mathbf{s}}_n^{(u)} = \left(\bar{s}_{n,0}^{(u)}, \bar{s}_{n,1}^{(u)}, \ldots, \bar{s}_{n,\eta-1}^{(u)}\right)^T$. Discarding the terms independent of symbols and states and taking into account that a CPM signal has a constant envelope, the joint distribution $p(\boldsymbol{\alpha}, \boldsymbol{\omega}, \boldsymbol{\psi}|\mathbf{r})$ can be factorized as

$$p(\boldsymbol{\alpha}, \boldsymbol{\omega}, \boldsymbol{\psi}|\mathbf{r}) \propto \left[\prod_{u=1}^{U} P\left(\omega_0^{(u)}\right) P\left(\psi_0^{(u)}\right)\right] \prod_{n=0}^{N-1} E_n(\boldsymbol{\alpha}_n, \boldsymbol{\omega}_n, \boldsymbol{\psi}_n) \tag{9}$$

$$\cdot \prod_{u=1}^{U} T_n^{(u)}\left(\alpha_n^{(u)}, \omega_n^{(u)}, \psi_n^{(u)}\right) G_n^{(u)}\left(\psi_{n+1}^{(u)}, \psi_n^{(u)}, \omega_n^{(u)}\right) I_n^{(u)}\left(\omega_{n+1}^{(u)}, \omega_n^{(u)}, \alpha_n^{(u)}\right) P\left(\alpha_n^{(u)}\right) \tag{10}$$

where

$$\begin{aligned}
I_n^{(u)}\left(\omega_{n+1}^{(u)}, \omega_n^{(u)}, \alpha_n^{(u)}\right) &= P\left(\omega_{n+1}^{(u)} \middle| \omega_n^{(u)}, \alpha_n^{(u)}\right) \\
G_n^{(u)}\left(\psi_{n+1}^{(u)}, \psi_n^{(u)}, \omega_n^{(u)}\right) &= p\left(\psi_{n+1}^{(u)} \middle| \psi_n^{(u)}, \omega_n^{(u)}\right) \\
T_n^{(u)}\left(\alpha_n^{(u)}, \omega_n^{(u)}, \psi_n^{(u)}\right) &= \exp\left\{\frac{1}{\Xi^2} \Re\left[\mathbf{r}_n^H \bar{\mathbf{s}}_n^{(u)} e^{\jmath\psi_n^{(u)}}\right]\right\} \\
E_n(\boldsymbol{\alpha}_n, \boldsymbol{\omega}_n, \boldsymbol{\psi}_n) &= \prod_{i=1}^{U-1} \prod_{k=i+1}^{U} \exp\left\{-\frac{1}{\Xi^2} \Re\left[\bar{\mathbf{s}}_n^{(i)H} \bar{\mathbf{s}}_n^{(k)} e^{-\jmath\left(\psi_n^{(i)} - \psi_n^{(k)}\right)}\right]\right\}.
\end{aligned} \tag{11}$$

Notice that $P\left(\omega_{n+1}^{(u)} \middle| \omega_n^{(u)}, \alpha_n^{(u)}\right)$ is an indicator function, equal to one if $\alpha_n^{(u)}$, $\omega_n^{(u)}$, and $\omega_{n+1}^{(u)}$ are compatible and to zero otherwise, and $p\left(\psi_{n+1}^{(u)} \middle| \psi_n^{(u)}, \omega_n^{(u)}\right) = p\left(\psi_{n+1}^{(u)} \middle| \psi_n^{(u)}, \alpha_{n-L+1}^{(u)}\right)$ is a Gaussian

DOI: 10.1002/sat

probability density function (pdf) in $\psi_{n+1}^{(u)}$ with mean $\left[\psi_n^{(u)} + \pi h \alpha_{n-L+1}\right]_{2\pi}$ and standard deviation σ_Δ. The FG corresponding to (10) has cycles of length four, that make unlikely the convergence of the SPA, since they are too short. We remove these short cycles by clustering the variables $\omega_n^{(u)}$ and $\psi_n^{(u)}$ and then stretching them in $\left(\alpha_n^{(u)}, \omega_n^{(u)}, \psi_n^{(u)}\right)$, obtaining a graph with shortest cycles of length twelve. Assuming, as in [6] that the interference among non-adjacent users is negligible, we approximate (11) as

$$E_n(\boldsymbol{\alpha}_n, \boldsymbol{\omega}_n, \boldsymbol{\psi}_n) \simeq \prod_{i=1}^{U-1} E_n^{(i,i+1)}\left(\alpha_n^{(i)}, \omega_n^{(i)}, \psi_n^{(i)}, \alpha_n^{(i+1)}, \omega_n^{(i+1)}, \psi_n^{(i+1)}\right) \qquad (12)$$

where

$$E_n^{(i,i+1)}\left(\alpha_n^{(i)}, \omega_n^{(i)}, \psi_n^{(i)}, \alpha_n^{(i+1)}, \omega_n^{(i+1)}, \psi_n^{(i+1)}\right) = \exp\left\{-\frac{1}{\Xi^2}\Re\left[\bar{\mathbf{s}}_n^{(i)H}\bar{\mathbf{s}}_n^{(i+1)} e^{-\jmath\left(\psi_n^{(i)}-\psi_n^{(i+1)}\right)}\right]\right\}.$$

This FG is shown in Figure 1 and is similar to that for the AWGN channel [6]. A major difference is represented here by the fact that continuous variables $\psi_n^{(u)}$ are now represented in the graph. Hence, the application of the SPA involves the computation of continuous pdfs and is not suited for a practical implementation. To overcome this problem, we may resort, as in [12], to the *canonical distribution* approach. Examples of commonly used canonical distributions for this channel can be found in [12]. In the numerical results, we will consider a canonical distribution composed of a weighted sum of impulses. In other words, each phase $\psi_n^{(u)}$ is quantized to D equally spaced values.

Although the algorithm has been obtained by assuming a Wiener PN with known incremental variance over a symbol interval, it can be employed even when the PN follows a different model. In this case, the value of σ_Δ^2 assumed at the receiver must be optimized by simulation for the PN at hand. In any case, there is in general a benefit from using at the receiver a value of thermal noise variance σ^2 larger than the actual one. The rationale of this trick is the following: since there is an overconfidence in the computed messages, we can make the algorithm less confident simply by describing the channel as if it added more noise than it really does [20].

4.2. Data-aided multiuser fine frequency synchronization

The MUD algorithm described in this paper requires the knowledge of the amplitude $\sqrt{2E_S/T}$ (possibly different in case of users with different powers) and frequency values $f^{(u)}$ for each user.

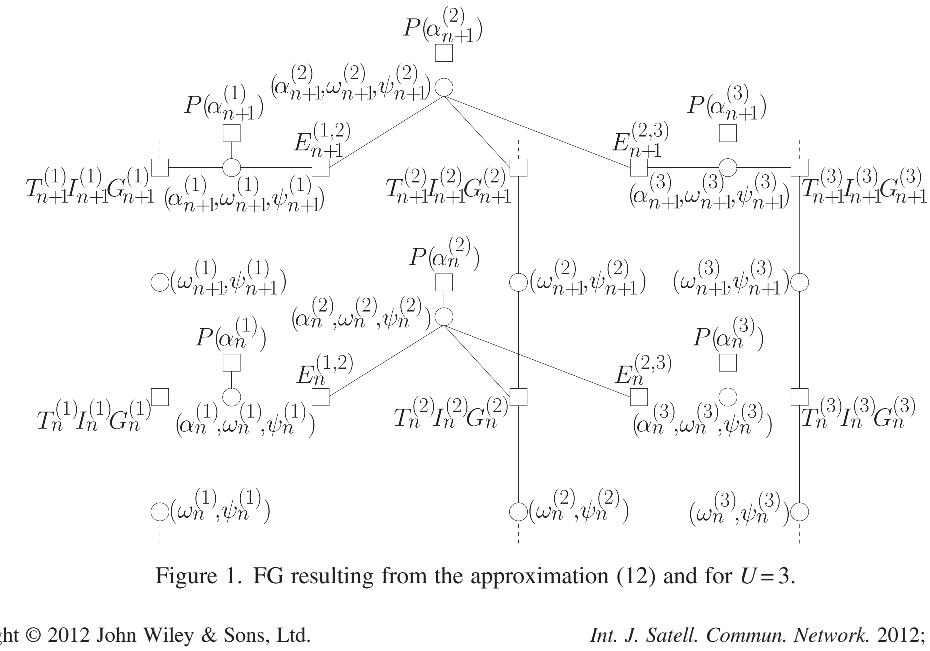

Figure 1. FG resulting from the approximation (12) and for $U = 3$.

DOI: 10.1002/sat

For them, we resort to DA estimation algorithms based on known-data fields usually inserted in the frame. Amplitude estimation is not an issue. In fact, the application of U occurrences of a DA maximum-likelihood single-user estimation algorithm provides amplitude estimates with a good accuracy for typical preamble lengths. Instead, DA single-user frequency estimation algorithms do not provide the required accuracy. This is obviously due to the interference of adjacent channels. For this reason, we employ interference cancellation to refine the estimates.

A first set of estimates of the frequency values $f^{(u)}$ is obtained by applying the DA algorithm in [21] to the preamble of each user. This algorithm does not require the knowledge of the channel phase for each user. These estimates are then iteratively refined still using the same single-user algorithm to the received signal after the contribution of the adjacent signals has been removed. To perform interference cancellation we need to employ not only the already estimated amplitude values and the frequency values of the previous iteration, but also the instantaneous (in case of a time-varying channel phase) values of the channel phase for each user. These are obtained by using the DA multiuser carrier phase estimation algorithm described in the next section, refined every time a new set of frequency estimates becomes available.

In summary, the algorithm proceeds as follows. The amplitude of each user is estimated first. Then, at each iteration a new set of frequency estimates is derived by using the single-user DA algorithm in [21] after the contribution of adjacent users has been removed. This set of frequency estimates is employed to perform DA multiuser carrier phase estimation whose output will be employed for interference cancellation at the next iteration.

A few iterations are in general sufficient, provided the known-data fields of all users have been properly optimized. The results shown in Section 5 refer to a properly designed optimization method, not discussed here for a lack of space.

4.3. Data-aided multiuser carrier phase estimation

We now describe a DA multiuser carrier phase estimation algorithm that requires the knowledge of the frequency and amplitude values of each user, estimated as described in the previous section. As mentioned, the phase estimates are used for interference cancellation necessary to improve the frequency estimates.

Let us assume a known-data field of P symbols ($K=\eta P$ samples). Defining $z_k=r_{n,m}, x_k^{(u)}=s_{n,m}^{(u)}$, and $\zeta_k=w_{n,m}$, with $k=n\eta+m$, we will assume that the known-data field corresponds to values $k=0,1,\ldots,K-1$. We also remove the hypothesis that the PN is constant over a symbol interval and define $\varphi_k^{(u)}=\theta^{(u)}(kT/\eta)$. Hence, we may express

$$z_k=\sum_{u=1}^{U}x_k^{(u)}\left(e^{\jmath\varphi_k^{(u)}}\right)+\zeta_k. \tag{13}$$

Let us define $\boldsymbol{\varphi}_k=\left(\varphi_k^{(1)},\ldots,\varphi_k^{(U)}\right)^T$, $\boldsymbol{\varphi}=\left(\boldsymbol{\varphi}_0^T,\ldots,\boldsymbol{\phi}_{K-1}^T\right)^T$ and $\mathbf{z}=(z_0,\ldots,z_{K-1})^T$. As before, we model the PN as a discrete-time Wiener process with incremental standard deviation over a symbol interval σ_Δ. We derive the MAP DA phase estimator:

$$\hat{\varphi}_k(u)=\arg\max_{\varphi_k^{(u)}}p\left(\varphi_k^{(u)}\middle|\mathbf{z}\right)\qquad u=1,\ldots,U,\quad k=0,\ldots,K-1.$$

Pdfs $p\left(\varphi_k^{(u)}\middle|\mathbf{z}\right)$ are obtained from $p(\boldsymbol{\varphi}|\mathbf{z})$ by using the FG/SPA framework. From (13), we may express

$$\begin{aligned}p(\boldsymbol{\varphi}|\mathbf{z})\propto p(\mathbf{z}|\boldsymbol{\varphi})p(\boldsymbol{\varphi})&=\prod_{k=0}^{K-1}\left[p(z_k|\boldsymbol{\varphi}_k)\prod_{u=1}^{U}p\left(\varphi_k^{(u)}\middle|\varphi_{k-1}^{(u)}\right)\right]\\&=\prod_{k=0}^{K-1}\left[p(z_k|\boldsymbol{\varphi}_k)\prod_{u=1}^{U}D_{k,k-1}^{(u)}\left(\varphi_k^{(u)}-\varphi_{k-1}^{(u)}\right)\right]\end{aligned} \tag{14}$$

DOI: 10.1002/sat

where $D_{k,k-1}^{(u)}\left(\varphi_k^{(u)}-\varphi_{k-1}^{(u)}\right)=p\left(\varphi_k^{(u)}\middle|\varphi_{k-1}^{(u)}\right)$ is a Gaussian pdf with mean $\varphi_{k-1}^{(u)}$ and standard deviation $\sigma_\Delta/\sqrt{\eta}$, according to the Wiener model. Neglecting irrelevant multiplicative terms, we can further factorize

$$p(z_k|\boldsymbol{\varphi}_k)\propto\exp\left\{-\frac{1}{2\Xi^2}\left|z_k-\sum_{u=1}^{U}x_k^{(u)}e^{\jmath\varphi_k^{(u)}}\right|^2\right\}\propto\prod_{u=1}^{U}B_k^{(u)}\left(\varphi_k^{(u)}\right)\prod_{u=1}^{U-1}\prod_{v=u+1}^{U}C_k^{(u,v)}\left(\varphi_k^{(u)},\varphi_k^{(v)}\right)\quad(15)$$

having defined

$$\begin{aligned}B_k^{(u)}\left(\varphi_k^{(u)}\right)&=\exp\left\{\frac{1}{\Xi^2}\Re\left[z_kx_k^{(u)*}e^{-\jmath\varphi_k^{(u)}}\right]\right\}\\C_k^{(u,v)}\left(\varphi_k^{(u)},\varphi_k^{(v)}\right)&=\exp\left\{\frac{1}{\Xi^2}\Re\left[x_k^{(u)}x_k^{(v)*}e^{\jmath\left(\varphi_k^{(u)}-\varphi_k^{(v)}\right)}\right]\right\}.\end{aligned}\quad(16)$$

From (14) and (15), we finally obtain the relevant factorization of $p(\boldsymbol{\varphi}|\mathbf{z})$. Node $C_k^{(u,v)}$ in the resulting FG connects variable nodes $\varphi_k^{(u)}$ and $\varphi_k^{(v)}$. Since the interference between two non-adjacent users is much smaller than the interference between adjacent users, we consider only functions connecting adjacent variable nodes, i.e., functions $C_k^{(u,u+1)}$. The simplified FG is shown in Figure 2.

Due to the presence of cycles in the FG of Figure 2, the application of the SPA gives an iterative algorithm which provides proper approximations of pdfs $p\left(\varphi_k^{(u)}|\mathbf{z}\right)$. We adopt the *canonical distribution* approach and, as in [8], we model the messages represented in Figure 2 as Tikhonov pdf, i.e.,

$$\begin{aligned}p_{f,k}^{(u)}\left(\varphi_k^{(u)}\right)&=t\left(a_{f,k}^{(u)};\varphi_k^{(u)}\right)\\p_{b,k}^{(u)}\left(\varphi_k^{(u)}\right)&=t\left(a_{b,k}^{(u)};\varphi_k^{(u)}\right)\\p_{l,k}^{(u-1,u)}\left(\varphi_k^{(u)}\right)&=t\left(a_{l,k}^{(u-1,u)};\varphi_k^{(u)}\right)\\p_{r,k}^{(u+1,u)}\left(\varphi_k^{(u)}\right)&=t\left(a_{r,k}^{(u+1,u)};\varphi_k^{(u)}\right)\end{aligned}\quad(17)$$

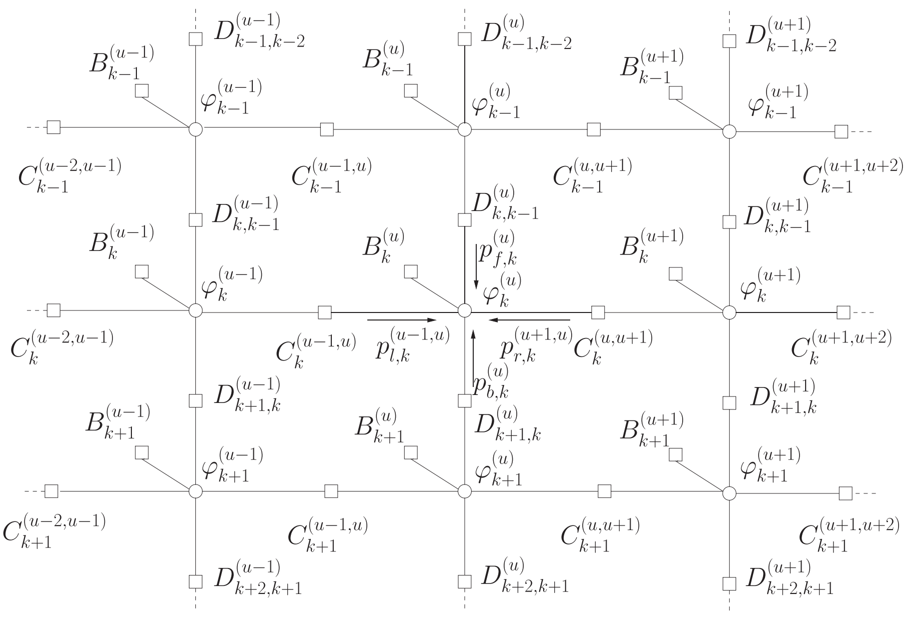

Figure 2. FG for the multiuser DA phase estimator.

where $t(\xi\,;x)$ is a Tikhonov distribution in x characterized by the complex parameter ξ:

$$t(\xi;x) = \frac{1}{2\pi \mathrm{I}_0(|\xi|)} \exp\left\{\Re\left[\xi e^{-jx}\right]\right\}$$

being $\mathrm{I}_0(\cdot)$ the zeroth-order modified Bessel function of the first kind. Hence, we simply have to update and propagate the complex parameters describing the Tikhonov pdfs. Let us first consider the update of parameter $a_{f,k}^{(u)}$. By generalizing the results in [8], we have

$$a_{f,k+1}^{(u)} = \gamma\left(a_{f,k}^{(u)} + \frac{z_k x_k^{(u)*}}{\Xi^2} + a_{l,k}^{(u-1,u)} + a_{r,k}^{(u+1,u)}, \frac{\sigma_\Delta}{\sqrt{\eta}}\right) \tag{18}$$

having defined $\gamma(\varepsilon,\zeta) = \frac{\epsilon}{1+|\epsilon|\zeta^2}$. Similarly,

$$a_{b,k-1}^{(u)} = \gamma\left(a_{b,k}^{(u)} + \frac{z_k x_k^{(u)*}}{\Xi^2} + a_{l,k}^{(u-1,u)} + a_{r,k}^{(u+1,u)}, \frac{\sigma_\Delta}{\sqrt{\eta}}\right). \tag{19}$$

Regarding parameters $a_{l,k}^{(u-1,u)}$ and $a_{r,k}^{(u+1,u)}$ we have

$$a_{l,k}^{(u,u+1)} = \delta\left(a_{f,k}^{(u)} + a_{b,k}^{(u)} + \frac{z_k x_k^{(u)*}}{\Xi^2} + a_{l,k}^{(u-1,u)}, \frac{x_k^{(u)} x_k^{(u+1)*}}{\Xi^2}\right) \tag{20}$$

and

$$a_{r,k}^{(u,u-1)} = \delta\left(a_{f,k}^{(u)} + a_{b,k}^{(u)} + \frac{z_k x_k^{(u)*}}{\Xi^2} + a_{r,k}^{(u+1,u)}, \frac{x_k^{(u-1)} x_k^{(u)*}}{\Xi^2}\right) \tag{21}$$

having defined $\delta(\epsilon,\zeta) = \frac{\epsilon\zeta}{\sqrt{|\epsilon|^2+|\zeta|^2}}$. In order to obtain (20) and (21), two approximations have been employed: $\mathrm{I}_0(|x|) \simeq e^{|x|}$ and $\sqrt{1+x} \simeq 1 + x/2$. The following schedule is adopted: messages $a_{f,k}^{(u)}$ and $a_{b,k}^{(u)}$ are first updated, for $k = 0, \ldots, K-1$ (with initial parameter $a_{f,0}^{(u)} = 0$) and $k = K-1, \ldots, 0$ (with initial parameter $a_{b,K-1}^{(u)} = 0$), respectively. Then messages $a_{l,k}^{(u-1,u)}$ and $a_{r,k}^{(u+1,u)}$ are updated for $u = 2, \ldots, U$ and $u = U-1, \ldots, 1$, respectively. A couple of iterations are, in general, sufficient. Finally, the estimates are

$$\hat{\varphi}_k^{(u)} = \arg\left(a_{f,k}^{(u)} + a_{b,k}^{(u)} + a_{l,k}^{(u-1,u)} + a_{r,k}^{(u+1,u)} + \frac{z_k x_k^{(u)*}}{\Xi^2}\right). \tag{22}$$

5. NUMERICAL RESULTS

For a lack of space, we limit our investigation to binary CPM formats. This choice is justified by the need to illustrate the relevant concepts and by the results which show that we can design transmission schemes with a very high efficiency using simple CPMs. We consider binary CPMs with $h = 1/3$, $L = 2$, and rectangular (REC) or raised-cosine (RC) frequency pulse. These schemes turned out to be the best ones among those considered.

5.1. Information-theoretic analysis

Figure 3 shows the SE as a function of the normalized spacing FT for the considered CPM formats and $E_s/N_0 = 10$ dB. In particular, we computed the achievable SE when a multiuser detector for different values of U' is employed. Note that curves with $U' = 1$ in practice refer to the use of a single-user detector. For each considered CPM scheme, a MUD strategy allows to achieve a higher SE than that achievable by a single-user detector and the frequency spacing which maximizes the SE is also lower in the MUD case.

As discussed in [4], the optimal spacing depends on the considered value of E_s/N_0 (although this dependence is quite smooth). Hence, according to the operating E_s/N_0, we choose the optimal

DOI: 10.1002/sat

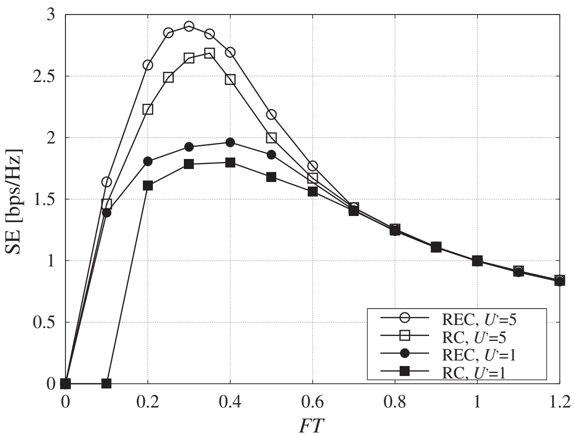

Figure 3. Spectral efficiency as a function of the normalized spacing for different values of U' at $E_s/N_0 = 10$ dB.

modulation format and the corresponding optimal spacing. For the REC scheme, $FT = 0.3$ (resp. 0.4) is the optimal spacing at $E_s/N_0 = 10$ dB when $U' = 5$ (resp. $U' = 1$), whereas $FT = 0.35$ (resp. 0.4) is that for RC when $U' = 5$ (resp. $U' = 1$). From Figure 3, we can also observe that the scheme with REC frequency pulse leads to a higher SE than the RC-based counterpart. The same conclusion can be drawn from Figure 4, where we consider the channel spacings resulting from the previous optimization and we plot the SE as a function of E_b/N_0, being E_b the energy per information bit. The figure shows that REC and RC formats perform similarly for low values of SE. However, REC allows achieving a higher SE.

5.2. BER performance

In the following, we will consider the design of a practical scheme based on the REC frequency pulse with a SE of 2.66 bps/Hz, slightly lower than the maximum achievable. There are several reasons for which we may expect a performance loss with respect to the information-theoretical results. Among these, the most important are the use of a finite-length code and the suboptimality of the adopted reduced-complexity receiver. From Figure 4, we observe that the achievable IR threshold in E_b/N_0 corresponding to a SE of 2.66 bps/Hz is about 7.6 dB. To obtain this SE, we concatenate, through an interleaver, the REC scheme with spacing $FT = 0.3$ with a (64,51) outer extended Bose, Ray-Chaudhuri, Hocquenghem (eBCH) code with rate $\rho = 0.8$ described in [22].

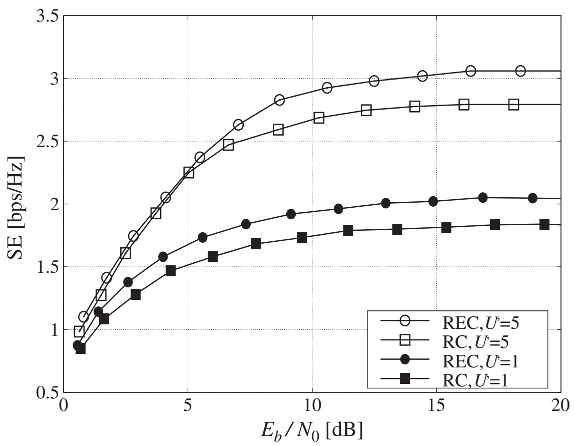

Figure 4. Spectral efficiency as a function of E_b/N_0, for channel spacings resulting from the optimization at $E_s/N_0 = 10$ dB.

DOI: 10.1002/sat

We consider iterative receivers employing the described reduced-complexity multiuser detectors as inner soft-input soft-output detectors with a maximum of 25 iterations in all cases. The bit error rate (BER) performance for the middle user only is shown in Figure 5 versus E_b/N_0. We assume that the users are synchronous. However, we also carried out BER analysis in the asynchronous scenario observing the same performance as for the synchronous case. We do not report the performance of the optimal MUD scheme—see [6] for a performance comparison.

When $U=\infty$ and $U'=5$, thus in the same conditions used in the information-theoretic analysis (although with a different receiver) we considered codewords of length 64000 information bits and the AWGN channel. A convergence threshold of about $E_b/N_0 \simeq 9.2$ dB and BER of 10^{-5} for $E_b/N_0 \simeq 9.6$ dB are obtained, less than a couple of dB worse than predicted. We also show the performance for $U=U'=5$ and AWGN and PN channels—in the latter case a Wiener model with $\sigma_\Delta = 1$ degree has been considered and at the receiver $D=24$ has been adopted.

It is worth noticing that the DVB-RCS2 [14] standard considers several modulation & coding formats, where quaternary CPMs are serially concatenated with an outer convolutional code, reaching SEs up to 1.8 bps/Hz. Therefore the proposed binary schemes outperform in terms of SE the CPM schemes considered in DVB-RCS2.

5.3. Synchronization

For the above mentioned REC-based scheme we now consider the issue of frequency synchronization. The described multiuser frequency synchronization scheme results unbiased. Hence, in Figure 6 we

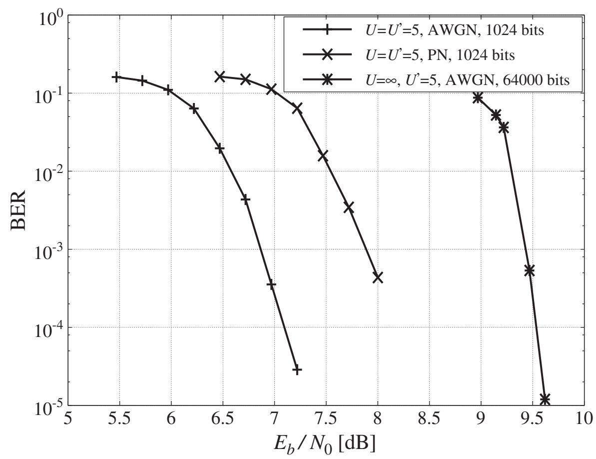

Figure 5. BER performance.

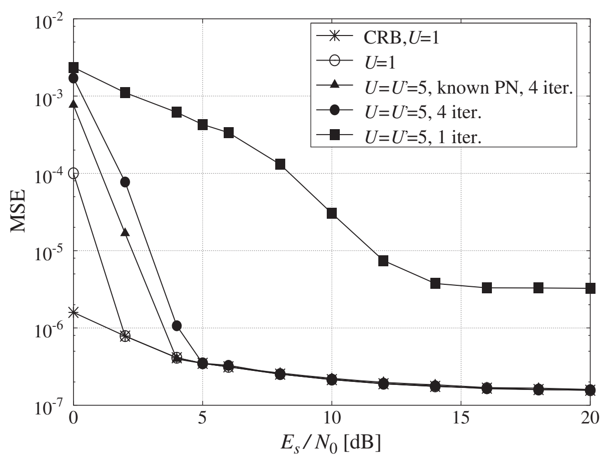

Figure 6. MSE of the multiuser frequency synchronization scheme in the presence of PN.

DOI: 10.1002/sat

show the mean square error (MSE) of the frequency estimate for the central user versus E_S/N_0, when $P=60$ symbols. A Wiener PN with $\sigma_\Delta = 1$ degree has been considered. As a reference curve, we show the Cramér-Rao lower bound (CRB) for a system with $U=1$, computed according to [23]. When $U=1$, this bound is reached by the frequency estimation algorithm in [21] for $E_S/N_0 \geq 2$ dB (curve with white circles). When $U=U'=5$ users are present, this algorithm gives a very poor performance (curve labeled “1 iteration” since it corresponds to the first iteration of the proposed multiuser algorithm). With 4 iterations we are able to reach, for $E_S/N_0 \geq 5$ dB, the CRB related to the presence of only one user. Hence, a very effective interference cancellation is performed. A slightly better result is obtained by using a genie-aided version of the proposed frequency synchronization algorithm in which the true values of the channel phases are employed for interference cancellation purposes. This is a proof of the effectiveness of the proposed DA multiuser carrier phase estimation algorithm described in Section 4.3.

6. CONCLUSIONS

We considered frequency division multiplexed systems based on continuous phase modulations. Through the information-theoretic analysis, we showed that it turns out more convenient to consider frequency spacings between the channels much lower than those usually employed to limit the interference from adjacent users, thus providing a better tradeoff between degradation of the information rate due to the interference and usage of the available spectrum. The limits predicted by the information theory can be approached by practical schemes based on the serial concatenation with a proper outer code.

We then proposed reduced-complexity schemes for multiuser detection, possibly in the presence of phase noise, and multiuser data-aided phase and frequency synchronization schemes. We showed that it is possible to implement transmission schemes with an unprecedented spectral efficiency at a price of a limited complexity increase with respect to a receiver which neglects the interference.

REFERENCES

1. Beidas BF, El Gamal H, Kay S. Iterative interference cancellation for high spectral efficiency satellite communications. *IEEE Trans Commun* 2002; **50**(1):31–36.
2. Gallinaro G, Rinaldo R. Assessment of potentiality of adjacent channel interference mitigation in a low-rate TDMA system. *Proc. Intern. Work. on Signal Processing for Space Commun*., Rhodes Island, Greece, 2008.
3. Barbieri A, Fertonani D, Colavolpe G. Time-frequency packing for linear modulations: spectral efficiency and practical detection schemes. *IEEE Trans Commun* 2009; **57**:2951–2959.
4. Barbieri A, Fertonani D, Colavolpe G. Spectrally-efficient continuous phase modulations. *IEEE Trans Wireless Commun* 2009; **8**:1564–1572.
5. Piemontese A, Graell i Amat A, Colavolpe G. Information-theoretic analysis and practical coding schemes for spectrally efficient FDM-CPM systems. *Proc. Intern. Symp. on Turbo Codes & Relat. Topics*, Brest, France, 2010.
6. Piemontese A, Colavolpe G. A novel graph-based suboptimal multiuser detector for FDM-CPM transmissions. *IEEE Trans Wireless Commun* 2010; **9**:2812–2819.
7. Kschischang FR, Frey BJ, Loeliger HA. Factor graphs and the sum-product algorithm. *IEEE Trans Inf Theory* 2001; **47**:498–519.
8. Colavolpe G, Barbieri A, Caire G. Algorithms for iterative decoding in the presence of strong phase noise. *IEEE J Sel Areas Commun* 2005; **23**(9):1748–1757.
9. Colavolpe G, Germi G. On the application of factor graphs and the sum-product algorithm to ISI channels. *IEEE Trans Commun* 2005; **53**:818–825.
10. Colavolpe G. On LDPC codes over channels with memory. *IEEE Trans Wireless Commun* 2006; **5**(7):1757–1766.
11. Barbieri A, Colavolpe G. Soft-output decoding of rotationally invariant codes over channels with phase noise. *IEEE Trans Commun* 2007; **55**(11):2125–2133.
12. Barbieri A, Colavolpe G. Simplified soft-output detection of CPM signals over coherent and phase noise channels. *IEEE Trans Wireless Commun* 2007; **6**(7):2486–2496.
13. Colavolpe G, Barbieri A. On MAP symbol detection for ISI channels using the Ungerboeck observation model. *IEEE Commun Lett* 2005; **9**(8):720–722.
14. Digital Video Broadcasting (DVB); Second Generation DVB Interactive Satellite System; Part 2: Lower Layers for Satellite standard. DVB Document A155-2, 2011.
15. Narayanan KR, Stüber GL. Performance of trellis-coded CPM with iterative demodulation and decoding. *IEEE Trans Commun* 2001; **49**:676–687.
16. Moqvist P, Aulin TM. Serially concatenated continuous phase modulation with iterative decoding. *IEEE Trans Commun* 2001; **49**:1901–1915.
17. Rimoldi BE. A decomposition approach to CPM. *IEEE Trans Inf Theory* 1988; **34**:260–270.

DOI: 10.1002/sat

18. Merhav N, Kaplan G, Lapidoth A, Shitz SS. On information rates for mismatched decoders. *IEEE Trans Inf Theory* 1994; **40**(6):1953–1967.
19. Arnold DM, Loeliger HA, Vontobel PO, Kavčic A, Zeng W. Simulation-based computation of information rates for channels with memory. *IEEE Trans Inf Theory* 2006; **52**(8):3498–3508.
20. Colavolpe G, Ferrari G, Raheli R. Extrinsic information in iterative decoding: a unified view. *IEEE Trans Commun* 2001; **49**:2088–2094.
21. Mengali U, Morelli M. Data-aided frequency estimation for burst digital transmission. *IEEE Trans Commun* 1997; **45**:23–25.
22. Graell i Amat A, Nour CA, Douillard C. Serially concatenated continuous phase modulation for satellite communications. *IEEE Trans Wireless Commun* 2009; **8**:3260–3269.
23. Barbieri A, Colavolpe G. On the Cramer-Rao bound for carrier frequency estimation in the presence of phase noise. *IEEE Trans Wireless Commun* 2007; **6**:575–582.

AUTHORS' BIOGRAPHIES

Amina Piemontese was born in San Giovanni Rotondo, Italy, in 1980. She received the Dr. Ing. degree in Telecommunications Engineering from the University of Parma, Parma, Italy, in 2006 and the Ph.D. degree in Information Technology from the University of Parma and from TELECOM Bretagne, Brest, France, in 2011. Currently, she holds a postdoctorate position at the University of Parma. Her research activity includes various topics in digital communications, with particular emphasis on iterative joint detection and decoding algorithms and multiuser communications theory.

Nicolò Mazzali was born in Carpi (MO), Italy, in 1983. He received the Dr. Ing. degree in Telecommunications Engineering (cum laude) in 2009 from the University of Parma, Parma, Italy. Currently, he is a Ph.D. student at Dipartimento di Ingegneria dell'Informazione (DII), University of Parma. His main research interests include digital transmission theory and information theory, with particular emphasis on iterative joint detection and decoding algorithms, estimation of unknown parameters and CPM-CDMA systems.

Giulio Colavolpe was born in Cosenza, Italy, in 1969. He received the Dr. Ing. degree in Telecommunications Engineering (cum laude) from the University of Pisa, in 1994 and the Ph.D. degree in Information Technologies from the University of Parma, Italy, in 1998. Since 1997, he has been at the University of Parma, Italy, where he is now an Associate Professor of Telecommunications at the Dipartimento di Ingegneria dell'Informazione (DII). In 2000, he was Visiting Scientist at the Institut Eur\'ecom, Valbonne, France. His research interests include the design of digital communication systems, adaptive signal processing (with particular emphasis on iterative detection techniques for channels with memory), channel coding and information theory. His research activity has led to more than 150 papers in refereed journals and in leading international conferences, and 15 industrial patents. He received the best paper award at the 13th International Conference on Software, Telecommunications and Computer Networks (SoftCOM'05), Split, Croatia, September 2005, the best paper award for Optical Networks and Systems at the IEEE International Conference on Communcations (ICC 2008), Beijing, China, May 2008, and the best paper award at the 5th Advanced Satellite Mobile Systems Conference and 11th International Workshop on Signal Processing for Space Communications (ASMS &SPSC 2010), Cagliari, Italy. He is currently serving as an Editor for IEEE Transactions on Wireless Communications and IEEE Wireless Communications Letters and as an Executive Editor for Transactions on Emerging Telecommunications Technologies (ETT).

DOI: 10.1002/sat